Influence of thermally radiative dissipative MHD flow of nanofluid past an exponentially stretching sheet

Shaik Mohammed Ibrahim

Department of Mathematics, Koneru Lakshmaiah Education Foundation, Vaddeswaram, Guntur, Andhra Pradesh- 522302, India

Email ID: ibrahim@kluniversity.in

Abstract:

In this work, I conducted a numerical investigation of the effects of viscous dissipation on the thermal radiation of a magneto-hydrodynamics (MHD) flow of an incompressible nano-fluid caused by an exponentially stretched sheet subject to heat and mass fluxes at the boundary layer. To numerically solve the governing PDEs, we first use self-similarity transformation to convert them into a set of ODEs, which we then solve using the shooting technique and a fourth-order Runge-Kutta method. The effects of a wide variety of limitations are demonstrated with respect to the non-dimensional flow, temperature, percentage of nano-particle capacity, and local Nusselt and Sherwood number. Calculated and analysed are the friction factor coefficient values, as well as the local Nusselt and Sherwood numbers.

Keywords: *Thermal Emission; MHD; Nanofluid; heat and mass fluxes; Viscous Dissipation.*

1. Introduction

The study of motion and heat transport over a stretched surface has gained a lot of attention in recent years due to its many applications, including persistent casting, exchangers, metal spinning, bundle wrapping, food processing, substance processing, and equipment, in addition to polymer extrusion. Crane was the first to investigate the Newtonian flowing flow produced by a stretched sheet [1]. Many researchers enhanced Crane's [1] work by taking into account the impact of mass transit in various contexts, such as Dutta et al. [2], Chen and Char [3], and Gupta [4]. Nadeem et al. [5] investigated the heat conduction property of a water-based nanofluid using the exponential stretched sheet. Bhattacharyya [6] looked at heat and mass conduction across a rapidly contracting sheet in the boundary layer.

Mukhopadhyay et al. [7] investigated the high-temperature transport flow through a permeable exponential stretched sheet with thermal radiation. Sajid and Hayat [8] investigated the implications of heat production on the boundary layer flow due to an exponentially stretched sheet. In the presence of velocity slip and a magnetic field, Zhang et al. [9] research focuses on the heat transport of a power law nanofluid thin film induced by a stretched sheet. Majeed et al.'s [10] demonstration of the boundary layer flow of ferromagnetic fluid across a stretched surface. Using an unsteady stretched sheet, Pal and Saha [11] looked into the heat and mass transfer in a thin liquid film under the impact of non linear thermal emission. Stretched surfaces were included in Weidman [12] investigation of a uniform formulation for stagnation point flows.

Modern metallurgical and metal-working processes use MHD flow of an electrically conductive fluid over a stretched sheet in unique manners. In order to cool them, continuous strips and filaments are frequently pulled from a moving fluid in professional polymer operations. The structure of the boundary layer adjacent to the stretched sheet influences the cooling rate, which greatly affects the outcome. Mukhopadhyay et al. [13] investigated the MHD flow of Casson fluid caused by an exponentially stretched sheet with heat emission. The impact of magnetohydrodynamics on a bidirectional nanofluid flow with a second-order slip flow and homogeneous-heterogeneous reactions has been examined by Hayat et al. in their study [14].

A stretched surface with internal heat generation was the subject of Lin et al.'s [15] investigation into the flow and heat transfer of an unstable MHD pseudo-plastic nanofluid in a finite thin film. To examine the impact of thermal radiation on the magnetohydrodynamics nanofluid flow and heat transfer, Sheikholeslami et al. [16] employed a two-phase model. On an MHD Falkner-Skan nanofluid stream, Farooq et al.'s [17] demonstration of the HAM-based Mathematica tool BVP h 2.0. In order to investigate the effects of thermal emission in a three-dimensional Jeffrey nanofluid stream with internal heat generation and magnetic field, Shehzad et al. [18] undertook an analytical investigation.

The significance of emission in processes carried out at extremely high temperatures cannot be emphasised. Radiative effects are used by gas turbines, missiles, aeroplanes, spacecraft, and nuclear power plants. The interaction of emission in a thermally convective viscous liquid stream across an inclined surface is studied by Moradi et al. [19]. The two phasemodel was utilised by Sheikholeslami et al. [20] to investigate the impact of emission in a viscous nanofluid stream. The laminar stream of an Oldroyd-B liquid with nanoparticles and emission is studied by Hayat et al. [21]. Ashraf et al. [22] conducted study on the radiative three-dimensional Maxwell fluid stream with thermophoresis and convective condition. The heat emission in a Powell-Eyring nanofluid laminar stream over a stretched sheet was studied by Hayat et al. [23].

The effect of thermal emission on the continuous laminar two-dimensional frontierlayer stream and heat transfer over an exponentially stretched sheet was studied by Bidin and Nazar [24]. Hady et al. [25] examined the effect of emission on viscous nanofluid over nonlinear stretched sheet using the Runge-Kutta fourth-order method. The effects of Joule heating and thermophoresis in a Maxwell model stretched stream under convection were examined by Hayat et al. [26]. Sakiadis stream of Maxwell fluid with convective frontiercondition is addressed by Mustafa et al. [27]. The Maxwell fluid's stagnation point stream in the presence of thermal emission and convection was examined by Hayat et al. [28]. The effects of an inclined magnetic field on heat generation in a nanofluid stream with non-linear thermal emission were examined by Hayat et al. [29]. The nonlinear radiative stream of a three-dimensional Burgers nanofluid is studied by Khan et al. [30] with a novel mass flux Prominence.

The goal of the current study is to numerically look into the impact of thermal emission on the magnetohydrodynamic (MHD) flow of a viscous incompressible nano-sized particle fluid appropriate to an exponentially stretched sheet with heat and mass fluxes conditions. The governing PDEs are converted into self-similar ODEs via similarity transformations and are then numerically solved via the Shooting technique.

2. Mathematical Formulation

A two-dimensional hydromagnetic flow of an incompressible fluid is modelled using an exponentially stretched sheet. Heat and mass transport analysis is characterized by the presence of thermal radiation, viscous dissipation, heat generation, and chemical reactions. A non-uniform magnetic field B(x) = B0exp(x/2l) is applied in the y-direction. In the case of low magnetic

Reynolds numbers, the contribution of the induced magnetic field is disregarded. Heated and mass flux boundary conditions were applied at the surface of the sheet. The following equations represent the fundamental principles of motion:

(i) Continuity:

$$\frac{\partial u}{\partial x}+\frac{\partial u}{\partial y}=0 \tag{1}$$

(ii) Momentum:

$$u\frac{\partial u}{\partial x}+v\frac{\partial u}{\partial y}=\nu\frac{\partial^2 u}{\partial y^2}-\frac{\sigma B_0^2}{\rho}u-\frac{\nu}{K^*}u \tag{2}$$

(iii) Energy:

$$u\frac{\partial T}{\partial x}+v\frac{\partial T}{\partial y}=\alpha\frac{\partial^2 T}{\partial y^2}+\frac{(\rho c)_p}{(\rho c)_f}\left[D_B\frac{\partial C}{\partial y}\frac{\partial T}{\partial y}+\frac{D_T}{T_\infty}\left(\frac{\partial T}{\partial y}\right)^2\right]-\frac{1}{\rho c_p}\frac{\partial q_r}{\partial y}+\frac{\mu}{\rho c_p}\left(\frac{\partial u}{\partial y}\right)^2 \tag{3}$$

(iv) Nanoparticle volume fraction:

$$u\frac{\partial N}{\partial x}+v\frac{\partial N}{\partial y}=D_B\frac{\partial^2 N}{\partial y^2}+\frac{D_T}{T_\infty}\frac{\partial^2 T}{\partial y^2} \tag{4}$$

subject to the frontier conditions:

$$u=U_w(x)=\mathrm{U}_0\exp\left(\frac{x}{l}\right),\ v=-V(x),$$
$$\frac{\partial T}{\partial y}=-\frac{q_w(x)}{\alpha},\ \frac{\partial N}{\partial y}=-\frac{q_{np}(x)}{D_B},\ \ at\ y=0 \tag{5a}$$

$$u\to 0,\ T\to T_\infty,\ N\to N_\infty,\ \text{as}\ y\to\infty \tag{5b}$$

Here u and v denote the stream mechanism in the x and y information respectively, ν a kinematic viscosity, $\alpha=\frac{k}{\rho c_p}$ a thermal diffusivity, k a fluid density, ρ a thermal conductivity, c_p a specific heat, T a fluid temperature, T_∞ a ambient temperature, N a fluid concentration, C_∞ a ambient concentration, $\alpha=k/\rho c_p$ a thermal diffusivity, k a thermal conductivity, c_p a specific heat, $q_r = \frac{16\sigma^* T_\infty^3}{3k^*}\frac{\partial T}{\partial Y}$ a radiative heat flux, k^* a mean absorption coefficient, σ^* a Stefan-Boltzmann constant, $(\rho c)_p$ a Prominence heat capacity of nanoparticles, $(\rho c)_f$ heat capacity of the base fluid. N is nanoparticle volume, D a mass diffusion $U_w(x) = \mathrm{U}_0 \exp\left(x/l\right)$ is a stretched stream of sheet, U_0 a reference stream, l a reference length, $q_w(x) = q_{w0}\,\mathrm{T}_0\sqrt{U_0/2\nu l}\,\exp\left(x/l\right)$ the variable heat flux, $q_{np}(x) = q_{np0}C_0\sqrt{U_0/2\nu l}\,\exp\left(x/l\right)$ a variable surface nanoparticle flux, U_0, T_0, q_{w0}, q_{np0}, N_0, are the reference stream, temperature and heat flux, surface nanoparticle flux, nanoparticle capacityfraction respectively, $V(x) = V_0\exp\left(x/l\right)$a special type of stream at the wall is considered (Bhattacharyya [30]) where V_0 is a constant. Here $V(x) > 0$ is the stream of suction and $V(x) < 0$is the stream of injection.

Introducing similarity transformations as follows:

$$\eta = y\left(\frac{U_0}{2\nu x}\right)^{1/2}\exp\left(\frac{x}{l}\right),\ \psi = \left(2\nu U_0 x\right)^{1/2} f\left(\eta\right)\exp\left(\frac{x}{l}\right),$$
$$u = U_0 f'\left(\eta\right)\exp\left(\frac{x}{l}\right),\ v = -\sqrt{\frac{\nu U_0}{2l}}\exp\left(\frac{x}{l}\right)\left[f\left(\eta\right) - \eta f'\left(\eta\right)\right], \tag{6}$$
$$T = T_\infty + \frac{q_{w0}}{\alpha}T_0\exp\left(\frac{x}{l}\right)\theta\left(\eta\right), C = C_\infty + \frac{q_{np0}}{\alpha}C_0\exp\left(\frac{x}{l}\right)\phi\left(\eta\right)$$

If the dimensional stream function $\psi(x,y)$ then $u = \frac{\partial\psi}{\partial y}$ and $u = -\frac{\partial\psi}{\partial x}$.

The continuity equation is automatically satisfied and using similarity transformation, the system of Eqs. (2), (3) and (4) becomes:

$$f''' + ff'' - 2f'^2 - (Ha + K)f' = 0 \tag{7}$$
$$\left(1 + \frac{4}{3}R\right)\theta'' + \Pr\left(f\theta' + f'\theta + N_b\theta'\phi' + N_t\theta'^2\right) + \Pr Ec\left(f''\right)^2 = 0 \tag{8}$$
$$\phi'' + Le(f\phi' - f'\phi) + \frac{N_t}{N_b}\theta'' = 0 \tag{9}$$

Here primes mean differentiation with respect to η, $Ha=\dfrac{\sigma B_0^2(x)l}{\rho U_w(x)}$ is a Hartmann numbers, $\Pr=\dfrac{\nu}{\alpha}$ is a Prandtl numbers, $R=\dfrac{4\sigma^* T_\infty^3}{kk^*}$ is a emission constraint and $Le=\dfrac{\nu}{D_B}$ is a Lewis numbers, $N_b=\dfrac{(\rho c)_p\, q_{np0}}{(\rho c)_f\, \nu}N_0$ is a Brownian motion constraint, $Ec=\dfrac{U_0^2}{T_0\rho c_p}$ is a Eckert numbers, and $N_t=\dfrac{D_T}{T_\infty}\dfrac{(\rho c)_p\, q_{w0}}{(\rho c)_f\, \alpha\nu}T_0$ is a thermophoresis constraint, respectively.

The transformed frontier conditions (5a) and (5b) are given by

$$\begin{aligned} &f(0)=S,\; f'(0)=-1,\; \theta(0)=-1,\; \phi(0)=-1 \\ &f'(\infty)=0,\; \theta(\infty)=0,\; \phi(\infty)=0 \end{aligned} \qquad (10)$$

Where $S=\dfrac{-v_0}{\sqrt{\nu c/2l}}$ is suction/injection constraint. Here the constraint is positive $S>0$ ($v_0<0$) for mass suction and negative $S<0$ ($v_0>0$) for mass injection.

The substantial quantities of concern are the confined skin friction coefficient, the wall heat transport coefficient (or the confined Nusselt numbers) and the wall deposition flux (or the confined Stanton numbers) which are defined as respectively where the skin friction C_f, the heat transport $q_w(x)$ and the mass transport Sh_x from the wall are given by

$$\sqrt{2C_f \operatorname{Re}_x}=f''(0),\; C_f=\frac{u}{U_w \exp(x/l)}\left(\frac{du}{dy}\right)_{y=0}, \qquad (11)$$

From the temperature field, we can study the rate of heat transport which is given by

$$\frac{Nu_x}{\sqrt{\operatorname{Re}_x}}=-\sqrt{\frac{x}{2l}}\left(1+\frac{4}{3}R\right)\theta'(0), Nu_x=-\frac{x}{(T_w-T_\infty)}\left(\frac{\partial T}{\partial y}\right)_{y=0} \qquad (12)$$

From the concentration field, we can study the rate of mass transport which is given by

$$\frac{Sh_x}{\sqrt{\operatorname{Re}_x}}=-\sqrt{\frac{x}{2l}}\phi'(0),\; Sh_x=-\frac{x}{(C_w-C_\infty)}\left(\frac{\partial C}{\partial y}\right)_{y=0} \qquad (13)$$

where $\operatorname{Re}_x=U_0 x/\nu$ the confined Reynolds numbers.

3. Method of solution:

The structure of ordinary differential equations (7) – (9) subject to the frontier conditions (10) are solved numerically using Runge–Kutta fourth-order integration with shooting technique. A step size of $\Delta\eta = 0.01$ was selected to be satisfactory for a convergence criterion of 10^{-6} in all cases. The grades are obtainable graphically in Figs. (1) –(7) and conclusions are drawn for stream field and other physical quantities of interest that have noteworthy Prominences.

4. Results and discussion:

Numerical solutions to Eqs. (7)–(9) with frontier conditions (10) are provided in Figs. (1)–(9) using the Runge-Kutta fourth-order integration with shooting method. (7). Ha = 1.0, S = 3.0, Le = 1.3, R = 0.1, Pr = 0.71, Ec = 0.1, Nt = 0.8, and Nb = 0.5 are the leading restrictions that are held constant throughout the computations. Suction constraint Hartmann numbers, Eckert numbers Ec, Lewis numbers Le, emission constraint R, thermophoresis numbers Nt, and Brownian motion constraints Nb all have an impact on the stream, temperature, and friction profiles of nano-sized particles. In Figures 1(a) and (b), we see the profiles of the stream, temperature, and nanoparticle capacityfriction for different values of the suction constraint.
As can be seen in Fig. 1(a), when the suction constraint is raised, the stream profiles go up. when can be seen in Figure 1(b), the temperature decreases when the suction constraint is tightened. Frictional profiles of streams, temperatures, and nanoparticles, as a result of the Hartmann numbers (i.e. the magnetic field constraint Ha), are displayed in Figs. 2(a) and (b). As demonstrated in Fig. 2(a), the stream patterns increase as Hartmann numbers are increased. Physically increasing the magnetic field also increases the Lorentz force. When greater force is used to stop the flow of a fluid, the fluid's velocity increases. As can be seen in Fig. 2(b), as the Hartmann numbers increases, the temperature decreases.

Figure 3(a) and (b) display the effects of the dissipative constraint, Eckert numbers Ec, on the stream and temperature profiles. As the dissipation constraint Ec is raised, the stream and temperature profiles of the stream are shown to expand. Generally speaking, higher viscosities result in higher stream profiles because their enhanced heat conductivity. Figure 4(a)-(b) displays the results of the thermophoresis constraint Nt on the temperature and the nano-particle capacity percent. As shown in Figure 4(a), as the thermophoresis constraint is tightened, both the temperature and nano-particle capacity fraction profiles rise. The thermophoresis constraint Nt is defined as the ratio of the nanoparticle diffusion rate to the thermal diffusion rate in the nanofluid.

As Nt increases, the thermal boundary layer grows because of the increasing temperature difference between the sheet and the fluid. As Nt grows, the thermophoresis force grows, and the nano-particle can move from hot to cold areas. This movement results in an increase in the capacity fraction of nano-particles. Figure 5(a)-(b) displays the effect that the emission constraint R has on the temperature and nano-particle capacity fraction profiles. It's important to remember that a better temperature profile results from a higher R value. This is because the average absorption coefficient drops with increasing R. As can be shown in Fig. 5(b), the fractional capacity of nanoparticles rises with increasing R.

Finally, the impact of the Lewis numbers Le and the Brownian motion constraint Nb on the capacity fraction profiles of nano-particles is depicted in Figs. (6) and (7). when can be seen in Fig. (6), when the Lewis numbers improves, the distribution of the nano-particle capacity fraction narrows. This is because the Brownian diffusion coefficient Nb drops with increasing Le, making it harder for nano-particles to disperse throughout the fluid. Therefore, the capacity percentage of nano-particles decreases as the Lewis statistic Le increases. In addition, the fractional capacity of nanoparticles in the profile falls as the Brownian motion constraint Nb is increased. The thermal boundary layer may become more substantial as a result of this. The physical mechanism by which an increase in Brownian motion decreases the concentration inside the frontier layer is an increase in nano-particle diffusion.

Data on the friction factor term, Nusselt numbers, and Sherwood numbers are shown mathematically in Tables 1 and 2, respectively. According to Table 1, increasing either the Nusselt numbers N or the Eckert numbers Ec results in a decrease in the skin friction coefficient. According to Table 2, the confined Nusselt and Sherwood numbers decrease as the significance of Ha increases, while the opposite is true for higher values of S.

Table 1: **S**tatistical values of friction factor term and confined Nusselt numbers for different values of *Ec* and *R* when *Ha*=2.0, *Nt*=0.5, *Nb*=0.8, *Pr*=0.73, *R*=0.5, *Ec*=0.5 and *Le* = 1.5.

Constraints(fixed values)	Constraints	$f''(0)$	$\mathrm{Re}_x^{-1/2}\, Nu_x$
Nt=0.5, *Nb* = 0.8, *S*=5.0, *Pr*=0.73, *R*=0.5, *Le*=1.5	*R*=0.20	1.2205578	0.560558
	0.25	1.216655	0.566655
	0.30	1.197775	0.567775
	Ec=0.0	1.265308	0.559308
	0.3	1.220558	0.560558
	0.5	1.208727	0.568727

Table 2: Numerical values of confined Nusselt numbers and confined Sherwood numbers for different values of *Ha* and *S* when *Ha*=2.0, *Nt*=0.5, *Nb*=0.8, *Pr*=0.73, *R*=0.5, *Ec*=0.2 and *Le* = 1.5.

Constraints(fixed values)	Constraints	$\mathrm{Re}_x^{-1/2}\, Nu_x$	$\mathrm{Re}_x^{-1/2}\, Sh_x$
Nt=0.5, *Nb* = 0.8, *S*=5.0, *Pr*=0.73, *R*=0.5, *Le*=1.5	*Ha*=2.0	0.551146	0.394789
	2.5	0.538588	0.387825
	3.0	0.503747	0.367843
	S=0.1	0.515308	0.351434
	0.3	0.523404	0.362578
	0.5	0.540727	0.378441

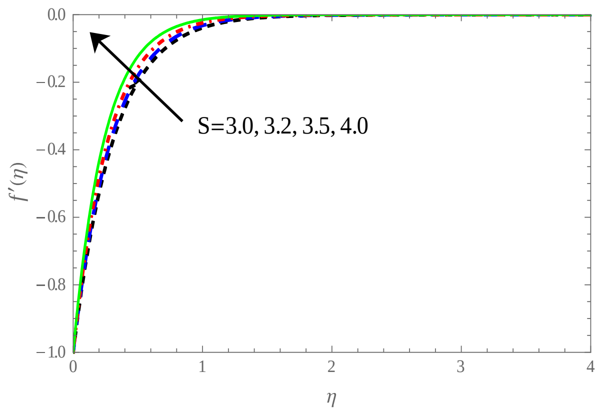

Fig 1(a). Prominence of s on $f'(\eta)$

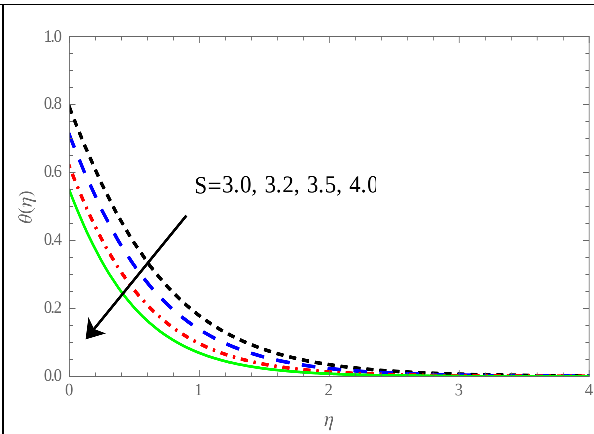

Fig 1(b). Prominence of s on $\theta(\eta)$

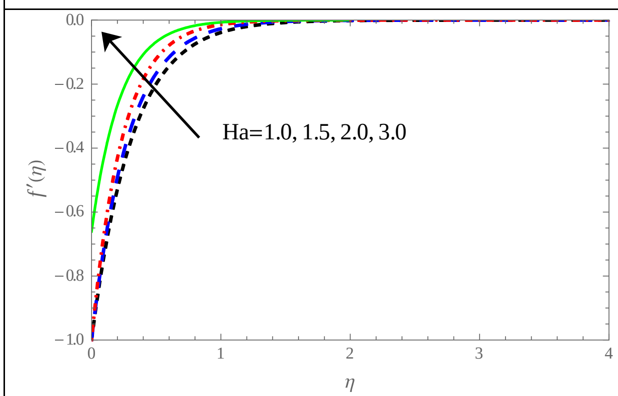

Fig 2(a). Prominence of Ha on $f'(\eta)$

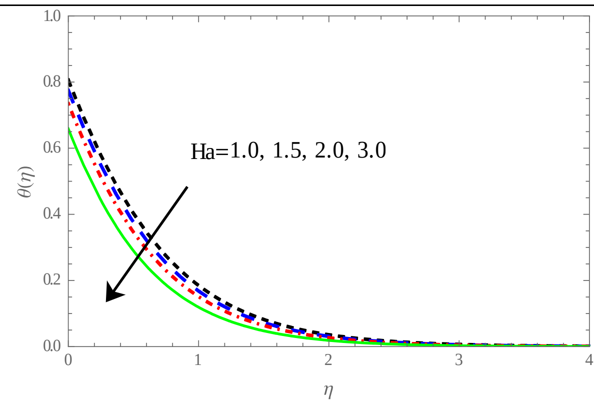

Fig 2(b). Prominence of Ha on $\theta(\eta)$

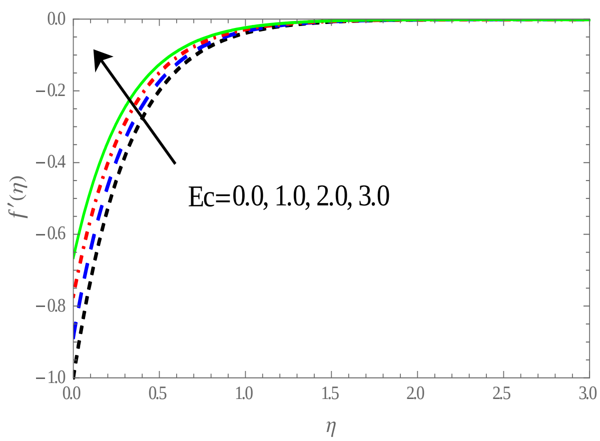

Fig 3(a). Prominence of Ec on $f'(\eta)$

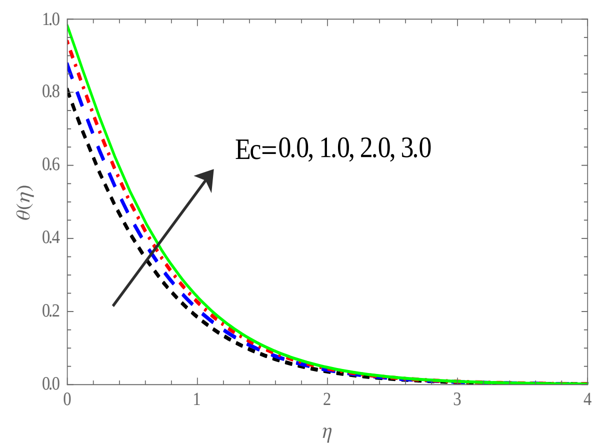

Fig 3(b). Prominence of Ec on $\theta(\eta)$

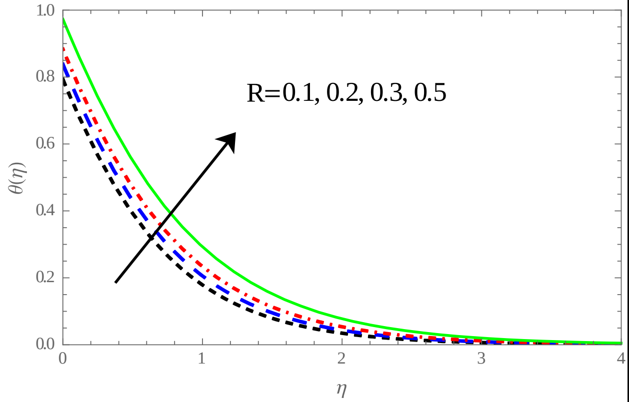

Fig 4(a). Prominence of R on $\theta(\eta)$

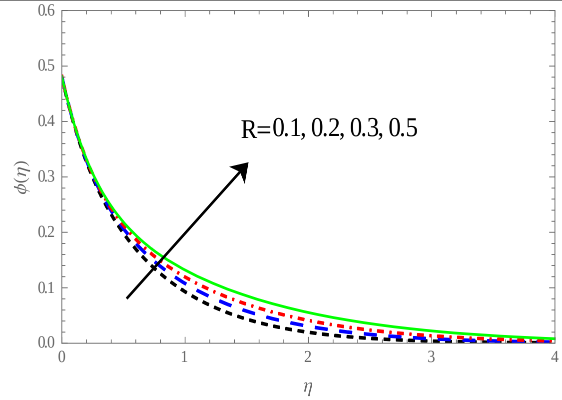

Fig 4(b). Prominence of R on $\phi(\eta)$

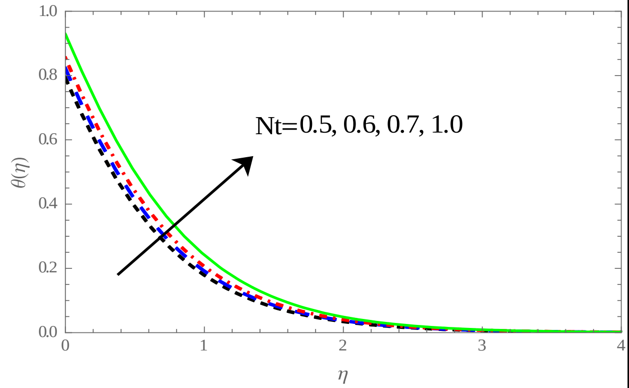

Fig 5(a). Prominence of Ec on $\theta(\eta)$

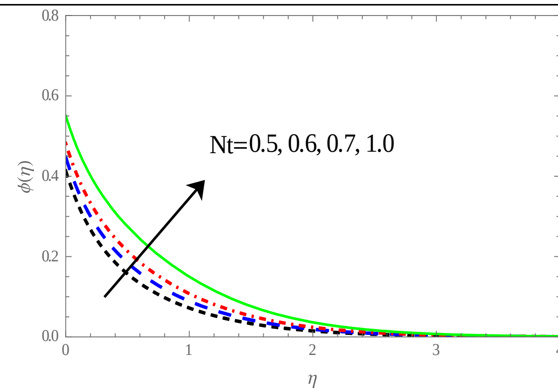

Fig 5(b). Prominence of Ec on $\phi(\eta)$

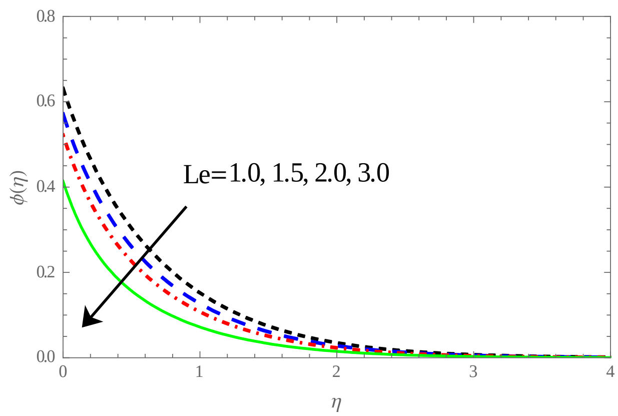

Fig 6. Prominence of Le on $\phi(\eta)$

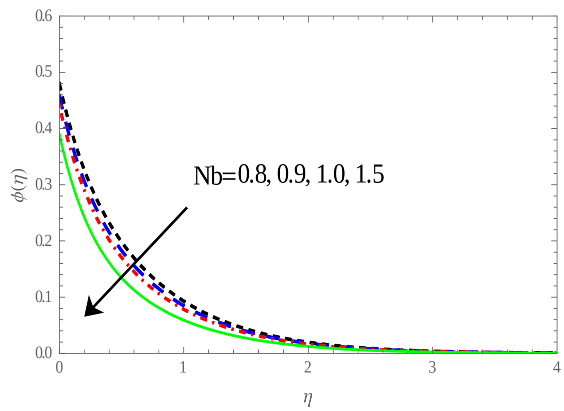

Fig 7. Prominence of Nb on $\phi(\eta)$

Conclusion:

Heat transport study employing an exponentially starching sheet under warm and mass flux circumstances with viscous dissipation is described, as is the significance of thermal emission and Magneto-hydro-dynamics (MHD) in the stream of a viscous dissipating nanofluid. The initial set of leading partial differential equations was transformed into a system of nonlinear coupled ordinary differential equations, and the resulting well-posed frontier value issue was solved numerically with the Runge-Kutta fourth order based shooting method. Relevant limitations on the fields of friction, skin friction, heat, and mass transport coefficients in relation to stream, temperature, and nano-particles are discussed and illustrated with graphs and tables. The study drew the following main results.:

(i) The suction constraint causes the stream profile and frontier layer thickness to grow. The Hartmann Numbers The Eckert-Harrington numbers Ec.

(ii) Larger suction constraints and Hartmann numbers lead to a lower temperature profile and thinner thermal boundary layer. Ha, but the emission parameter R and Eckert numbers Ec both go down as their values rise.

(iii) When the radiation constraint R and the thermophoresis constraint Nt are both high, the nano-particle capacity fraction rises.

(iv) As the values of R and Ec are constrained, the skin fraction coefficient decreases.

(v) Local Nusselt numbers is increasing function of S, R and Ec.

(vi) Local Sherwood numbers is increasing function of S.

References:

[1] Crane, L .J.,(1970). Stream past a stretched plate. Zeitschrift für angewandte Mathematik und Physik *ZAMP*, 21(4), 645–647.

[2] Dutta, B. K, Roy P, Gupta, A.S.(1985). Temperature field in flow over a stretched sheet with uniform heat flux. *Int Commun Heat Mass Transport* ,12(1):89–94.

[3] Char, M.I. (1988). Heat transport of a continuous, stretched surface with suction or blowing. *J Math Anal Appl.,* 135(2):568–80.

[4] Gupta ,P.S., and Gupta, A.S., (1977). Warm and mass transport on a stretched sheet with suction or blowing. *Can J Chem Eng,* 55(6):744–746.

[5] Nadeem S, Haq R.U., and Khan Z .H.,(2014). Heat transport analysis of water-based nanofluid over an exponentially stretched sheet. *Alexandria Eng. J.*, 53(1) pp. 219–224.

[6] Bhattacharyya, K., (2011)., Frontierlayer stream and heat transport over an exponentially shrinking sheet, *Chin. Phys. Lett.*, 28(7), 4701.

[7] Mukhopadhya S.,(2013). Slip Prominences on MHD Boundary layer stream over an exponentially stretched sheet with suction/blowing and thermal emission. *Ain Shams Eng J.*, 4(3):485–491.

[8]. Sajid, M., Hayat, T. (2008). Influence of thermal emission on the frontierlayer stream due to an exponentially stretched sheet, *Int. Commun. Heat Mass Transf.* 35, 347–356.

[9] Zhang, Y. Zhang, M, Bai Y.,(2017). Unsteady stream and heat transport of power-law nanofluid thin film over a stretched sheet with variable magnetic field and power-law stream slip Prominence, *J. Taiwan Inst Chem Eng*., 70:104–110.

[10] Majeed A, Zeeshan A, Ellahi R (2016). Unsteady ferromagnetic liquid stream and heat transport analysis over a stretched sheet with the Prominence of dipole and prescribed heat flux, *J Mol Liq* 223:528–533.

[11] Pal D, Saha P (2016). Influence of nonlinear thermal emission and variable viscosity on hydromagnetic warm and masstransport in a thin liquid film over an unsteady stretched surface. *Int J Mech Sci*, Vol. 119:208–216.

[12] Weidman P, Turner M R (2017). Stagnation-point streams with stretched surfaces: a unified formulation and new results. *Eur J Mech B Fluids*, 61, 144–153.

[13] S. Mukhopadhyay, I.C. Moindal, T. Hayat(2014). MHD frontierlayer stream of Casson fluid passing through an exponentially stretched permeable surface with thermal emission, *Chin. Phys*. B, 23 104701-12.

[14] T. Hayat, M. Imtiaz, A(2015). Alsaedi, Impact of magnetohydrodynamics in bidirectional stream of nanofluid subject to second order slip stream and homogeneous–heterogeneous reactions, *J. Magn. Magn. Mater.*, 395 294–302.

[15] Y. Lin, L. Zheng, X. Zhang, L. Ma, G. Chen(2015). MHD pseudo-plastic nanofluid unsteady stream and heat transport in a finite thin film over stretched surface with internal heat generation, *Int. J. Heat Mass Transf.*, 84 903–911.

[16] M. Sheikholeslami, D.D. Ganji, M.Y. Javed, R. Ellahi (2015). Prominence of thermal emission on magnetohydrodynamics nanofluid stream and heat transport by means of two phase model, *J. Magn. Magn. Mater.*, 374, 36–43.

[17] U. Farooq, Y.L. Zhao, T. Hayat, A. Alsaedi, S.J. Liao (2015). Application of the HAM-based Mathematica package BVPh 2.0 on MHD Falkner–Skan stream of nanofluid, *Comput. Fluids*, 11 69–75.

[18] S.A. Shehzad, Z. Abdullah, A. Alsaedi, F.M. Abbaasi, T. Hayat (2016). Thermally radiative three-dimensional stream of Jeffrey nanofluid with internal heat generation and magnetic field, *J. Magn. Magn. Mater.*, 397, 108–114.

[19] A. Moradi, H. Ahmadikia, T. Hayat, A. Alsaedi(2013). On mixed convection emission interaction about an inclined plate through a permeable medium, *Int. J. Thermal Sci.* 64,129–136.

[20] M. Sheikholeslami, D.D. Ganji, M.Y. Javed, R. Ellahi (2015). Prominence of thermal emission on magnetohydrodynamics nanofluid stream and heat transport by means of two phase model, *J. Mag. Magnetic Materials* 374, 36–43.

[21] Hayat T., T. Hussain, S. Shehzad, A. Alsaedi, A (2015). Stream of Oldroyd-B fluid with nanoparticles and thermal emission, *Appl. Math. Mech.* 36, 69-80.

[22] M. Ashraf, T. Hayat, S. Shehzad, A. Alsaedi(2015) Mixed convection radiative stream of three dimensional Maxwell fluid over an inclined stretched sheet in occurrence of thermophoresis and convective condition, *AIP Adv.* 5, 027134.

[23] Hayat T., N. Gull, M. Farooq, B. Ahmad (2015). Thermal emission Prominence in MHD stream of Powell-Eyring nanofluid induced by a stretched cylinder, *J. Aerospace Eng., ASCE*. 29(1),1943-5525.

[24] Bidin B and Nazar R(2009)., Numerical Solution of the FrontierLayer Stream over an Exponentially Stretched Sheet with Thermal Emission, Eur. J. Sci. Res. **33** (4), 710–717.

[25] Hady F.M, Ibrahim F.S, Abdel-Gaied S.M, Eid M.R (2012) Emission Prominence on viscous stream of a nanofluid and heat transport over a nonlinearly stretched sheet, *Nano Scale Res Lett* 7:299.

[26] Hayat T., M. Waqas, S.A. Shehzad, A. Alsaedi (2014). Prominences of Joule heating and thermophoresis on stretched stream with convective frontierconditions, *Scientia Iranica B* 21, 682–692.

[27] M. Mustafa, J. Khan, T. Hayat, A. Alsaedi(2015). Sakiadis stream of maxwell fluid considering magnetic field and convective frontierconditions, *AIP Adv.,* 5, 027106.

[28] Hayat T., M. Waqas, S. Shehzad, A. Alsaedi(2013). Mixed convection radiative stream of Maxwell fluid near a stagnation point with convective condition, *J. Mech.* 29, 403–409.

[29] Hayat T., S. Qayyum, A. Alsaedi, A. Shafiq(2016). Inclined magnetic field and heat source/sink aspects in stream of nanofluid with nonlinear thermal emission, *Int. J. Heat Mass Transport* 103, 99–107.

[30] Khan, M. Khan, W.A., Alshomrani, A.S. (2016). Non-linear radiative stream of three dimensional Burgers nanofluid with new mass flux Prominence, *Int. J. Heat Mass Transport*, 101, 570–576.